Case Western Reserve University

CSDS 399 - Final Report

Applying Kalman Filtering to Model Circadian Rhythms: A Novel Approach to Analyzing Wearable Sensor Data

Authors:
Asya Akkus, Siddharth Khadkikar, Ashley Sah, Ritika Devarakonda, Maisoon Rahman, & Noah Henriques

1 Introduction and Background

1.1 Overview of Biological Rhythms

The suprachiasmatic nucleus (SCN) is a small cluster of neurons in the brain that serves as an internal clock for the body's biological cycles. These cycles, called circadian rhythms, are measurable physiological changes an organism experiences over a 24-hour period. Examples of such measurable changes include the sleep-wake cycle, basal body temperature, hormone release, and appetite/digestion. The SCN coordinates and synchronizes these circadian rhythms across different organs and tissues and corrects deviations when they begin to drift (Ma & Morrison, 2024). Mapping and understanding the activity of the SCN in coordinating these cycles could provide valuable personalized health insights.

For example, by mapping basal body temperature over a 24-hour period, healthcare providers could gain insights into a person’s metabolic health, sleep quality, and reproductive function. Fluctuations in basal body temperature follow a predictable circadian pattern, typically peaking in the late afternoon and dipping during the night. Looking even further, mapping 24-hour circadian rhythms like kidney and liver function can predict the best times throughout the day to administer medication, such as chemotherapy. Timing treatments during periods of peak organ activity can maximize the body’s ability to process and eliminate drugs, thereby reducing side effects and improving efficacy. These concepts can be expanded to model other 24-hour clocks in the body, such as muscle strength, which often peaks in the late afternoon, and digestive activity, to provide further health insights.

1.2 Proposed Solution

We propose modeling the SCN activity using Kalman filtering, a recursive algorithm that uses its past states and noisy measurements to estimate the future state of a dynamic system one unit at a time. While there is literature on its ‘sub-systems’, such as CBT, modeling the SCN using Kalman filtering on wearable device data has not been thoroughly explored.

In the past, Kalman filtering has been applied to biological systems for modeling the central nervous system’s control of movement (Bieda). It has also been used to process and optimize time series data successfully. Due to this success in the biological and timing realms, it stands to reason that Kalman filtering can be implemented as a reasonable model for certain circadian rhythms (Asgari-Targhi & Klerman, 2019). Kalman filtering has also been successfully applied to sensor fusion, so it can be a good way to combine different biological clocks and produce a resultant time series with much greater accuracy and less uncertainty than either of the individual biological clocks taken separately. Given the ability of a Kalman filtering model to account for noise and different domains of features, applying this technique to modeling the SCN is worthy of exploration.

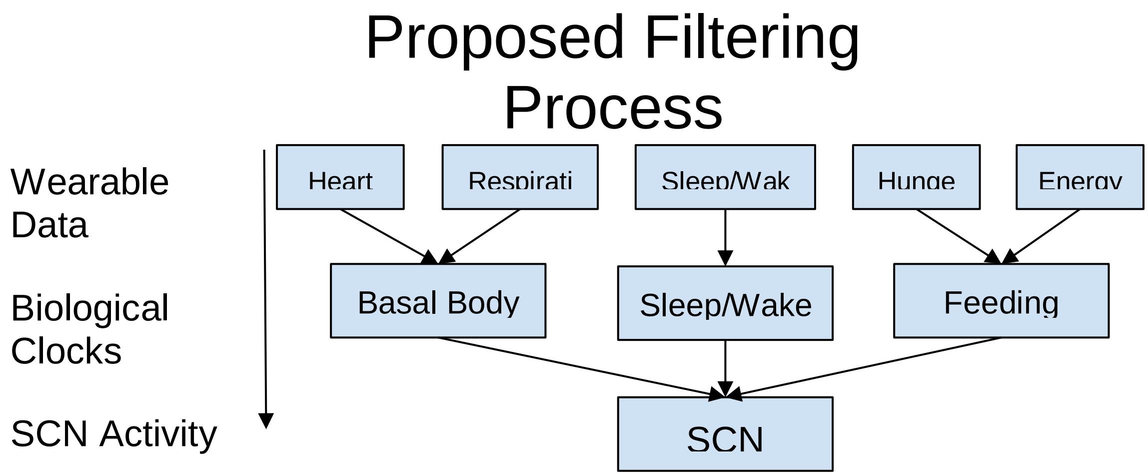

Figure 1: Filtering Process

Wearable, real-time data is collected. It is processed and ensembled to model individual biological clocks. For this proof of concept, basal body temperature, the sleep/wake cycle, and feeding behavior clocks will be modeled from the wearable data using Kalman filtering. From there, a higher-order Kalman filter will be used to combine the biological clocks generated in the previous step to create a model of SCN activity over time for the subject.

1.2a Kalman Filtering Algorithm Overview:

Many systems (including activity in the SCN) can be modeled in the following manner:

$$x_k = A_k x_{k-1} + B u_k + w_k$$
$$z_k = H x_k + v_k$$

Where A is the state transition matrix (from x_{k-1} to x_k), the Bu_k term pertains to set controls (in our application this is ignored), w_k is some process noise, H is the matrix relating the state to the measurement and v_k is the measurement noise.

The Kalman Filter estimates the process state at some time stamp k and then receives noisy measurements as feedback. The measurements are then incorporated into the state estimate. This divides Kalman filtering into two steps (1) the time-update or predict step and (2) the measurement update or correcting step.

This process is illustrated in the equations below:

Step-Update Equations:

$$\hat{x}_k = A x_{k-1} \qquad \text{, calculating the next state}$$
$$P_k^{-} = A P_{k-1} A^T + Q \text{, updating the error covariance}$$

Where A is the state transition matrix, P_k^{-} is the covariance in error of the state estimate prior to accounting for measurements and Q is a matrix accounting for additional uncertainty coming from outside factors we cannot measure.

Measurement Update Equations:

$$K_k = P_k^{-} H^T \left(H P_k^{-} H^T + R \right)^{-1}$$, calculating the Kalman gain

$$\hat{x}_k = \hat{x}_k^{-} + K_k \left(z_k - H \hat{x}_k^{-} \right)$$, updating the estimate with measurement z_k

$$P_k = \left(I - K_k H_k \right) P_k^{-}$$, updating the error covariance

Where H is the matrix relating the state to predicted measurements, R is the measurement error and K is the Kalman gain.

Outside disturbances, such as varying light levels, contribute to “noise” in an organism’s daily life and activities. The Kalman filter adjusts for these inputs, and adjusts to the different rhythms to maintain synchronization with external time cues such as the light-dark cycle or even the menstrual cycle (both of which can reasonably serve as a reference clock).

A Kalman filter, as has been claimed before, might be used to:

1. **Estimate the Phase of the Biological Clock:** By modeling the phase of the circadian rhythm as a dynamic system, the filter could estimate the current phase based on noisy measurements of environmental light and internal biological signals.
2. **Correct Deviations:** If the circadian rhythm deviates from the desired synchronization (e.g., due to jet lag or shift work), the Kalman filter could provide corrections by adjusting the predicted phase to realign with the environmental cycle.
3. **Adaptation to Noise:** The SCN has to adapt to irregular and noisy signals from the environment. Kalman filtering is well-suited for handling such noise, making it a potential tool for modeling how the SCN processes these signals to maintain synchronization.

1.3 Technical Project Requirements and Specifications

Below is a description of the technical project requirements and specifications for the scope of this project:

1. Data collection and preprocessing:
    a. Requirement: Collect internal biological signals (e.g. heart rate, VO2, core body temperature) with high temporal resolution.
    b. Details: The data preprocessing system must be robust, as irrelevant data must be filtered out, removing any outliers and noise before inputting it into the Kalman filter.
2. A working Kalman filter for each biological clock:
    a. Requirement: Implement separate working Kalman filters using data from the wearable device. Each working filter will represent basal body temperature, sleep/wake, and feeding behavior rhythms, respectively. Each filter should be capable of synchronizing multiple input data streams to estimate the phase of the circadian rhythm.
    b. Details: The filter must be adaptable to noise and disturbances and provide real time corrections.
3. Real-time synchronization of the biological clocks:
    a. Requirement: Ensure the Kalman filter and any other algorithms implemented, like the sensor fusion, operate in real-time, providing continuous updates and corrections.

    b. Details: The system should have low latency and high reliability, and there must be a system to check that so that accuracy can be maintained.
4. The visualization of the resulting biological clock:
    a. Requirement: Develop a user-friendly interface that allows users to visualize the current state of the biological clock, the estimated phase, and any corrections being applied by the Kalman filter.
    b. Details: The interface should provide clear, real-time feedback and be accessible to users with varying levels of technical expertise.
5. Validation of results:
    a. Requirement: Design a framework to validate the accuracy and reliability of the filter under varying scenarios that mimic real-world scenarios and quantify the accuracy.
    b. Details: Currently there is no way to quantitatively measure the accuracy of the Kalman filter graphs due to the scope of the project.
6. Documentation and reporting:
    a. Requirement: Maintain detailed documentation of the system architecture, algorithms, and testing procedures, along with regular progress reports.
    b. Details: Documentation should be clear, thorough, and accessible to facilitate future development, maintenance, or research based on this project.

2 Procedure

In the first half of the semester, much of our project progress was characterized by data processing, data cleaning, literature review of existing implementations of Kalman filtering in a biological context, and experimenting with different methods for Kalman filtering of the CBT.

In the second half of the semester, after we had worked on getting the CBT Kalman filter graph, we focused on tuning the matrices by reviewing available literature online, and then modeling our predicted hunger levels' Kalman filter and the ensemble Kalman filter graph based on the research for core body temperature. From there, we shifted our focus to ensembling the estimates from core body temperature and hunger levels to create our predicted suprachiasmatic nucleus activity.

2.1 Data Collection & Extraction

We collected raw data from an Apple Watch, initially exported in an XML format and converted to a CSV format. The dataset included metrics such as Heart Rate, Respiratory Rate, Basal Energy Burned, and Sleep Time. Using Python's csv.DictReader, we parsed the CSV files to extract relevant columns and processed the data into structured arrays. These arrays served as input for our Kalman filter models, providing a foundation for accurate analysis and refined predictions.

2.2 Data Aggregation and Interpolation

After data collection, we faced misaligned timestamps for metrics like heart rate, respiratory rate, and basal energy burned, captured at different intervals. To resolve this, we normalized all measurements to 1-minute intervals and used interpolation to fill gaps in the data. These steps ensured a continuous, synchronized time series, enabling accurate modeling of physiological patterns and the construction of reliable circadian clock models.

We focused on heart rate, respiratory rate, basal energy burned, sleep/wake status, and exertion rate for our Kalman filter model. Before modeling, we conducted exploratory data analysis (EDA) to understand trends and patterns. By generating visualizations for these metrics, we identified anomalies, observed distributions, and gained insights into variable behavior over time. This EDA informed our data structuring and optimization for Core Body Temperature (CBT) estimation.

value <chr>	count <int>
HKCategoryValueSleepAnalysisInBed	6677
HKCategoryValueSleepAnalysisAsleepCore	1148
HKCategoryValueSleepAnalysisAwake	671
HKCategoryValueSleepAnalysisAsleepREM	401
HKCategoryValueSleepAnalysisAsleepDeep	298
HKCategoryValueSleepAnalysisAsleepUnspecified	72

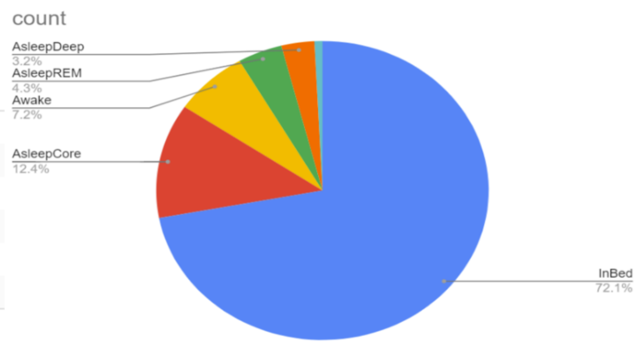

Figure 2: *Table showing the count for each sleep type (left), and percentage of time the subject is in the various stages of sleep (right).*

The table above on the left shows the count for each sleep value giving us a good idea of each category. The pie chart on the right visualizes this data in the table. The measurements for these sleep values are all taken at night, and the pie chart visualizes the percentage of time he is in bed, or awake, or in various stages of sleep during the total time of these measurements being taken at night.

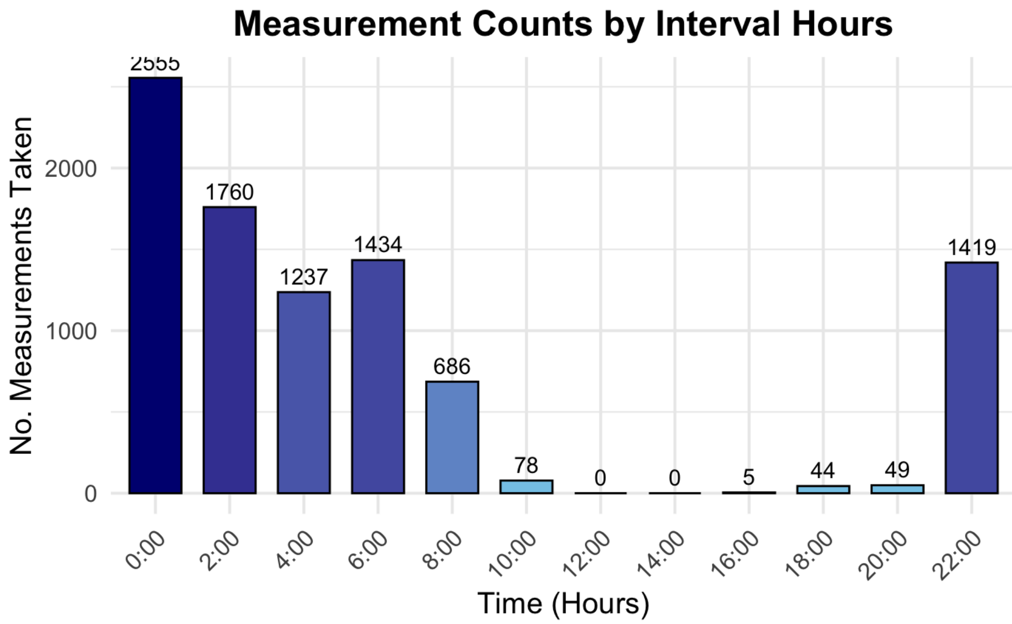

Figure 3: *Graph showing the time interval and the measurements at each time interval.*

The table above shows the time interval, and the measurements occurring during the time intervals. The measurements are higher during some increments because the Apple Watch is only taking measurements when the subject is asleep. So most of the measurements are only available for when he is asleep.

2.4 Initial Results with Implementation of the Kalman Filter

We successfully set up an initial Kalman Filter for CBT, which contained the following components:

- *State Transition Matrix (F):* This matrix governs how the state vector evolves from t to t+1. This matrix predicts the next state for CBT and HR based on current values. By eventually tuning the F matrix, we aim to accurately model how changes in heart rate and respiration rate drive fluctuations in core body temperature, something that is not reliably measured by many wearables.
- *Measurement Matrix (H):* The purpose of this matrix is to map the state vector to the measurement space. In the case of the CBT Kalman filter, it specifies how measurements of HR, RR, and basal body temperature are extracted from the state vector. Each row in the matrix defines a specific health data.
- *Covariance Matrices (P, Q, R):*
    - Initial Covariance Matrix (P): The P matrix was defined based on the variance of each state (CBT, HR, ST) at consistent time stamps. Our initial guess represents the uncertainty in the initial state estimates.
    - Process Noise Covariance Matrix (Q): This models the uncertainty or noise in the system dynamics. It represents the level of noise in the process model (i.e., how much we expect the actual system to deviate from the idealized state transition model).

- Measurement Noise Covariance Matrix (R): This models the noise or uncertainty in the measurements of HR, RR, and BBT. Each diagonal entry in the matrix represents the variance (noise) in the corresponding measurement.

2.4a Implementation of Kalman Filter of Core Body Temperature

In the development of our CBT Kalman Filter, we began by reviewing two foundational papers that explored different models for circadian rhythm estimation and noise reduction in physiological signals. These papers provided a solid starting point for understanding the dynamic systems involved in CBT regulation. Using the models from these papers, we generated two initial graphs. The first model, from Paper 1 (Ezequiel Juarez Garcia et al., 2022), yielded promising results, as shown in the graph below. The Simulated Heart Rate Data and Core Temperature Data from Kalman Filtering match closely in shape, as well as the Kalman filter graph having less noise, a key feature in proving that the model was somewhat close to being accurate.

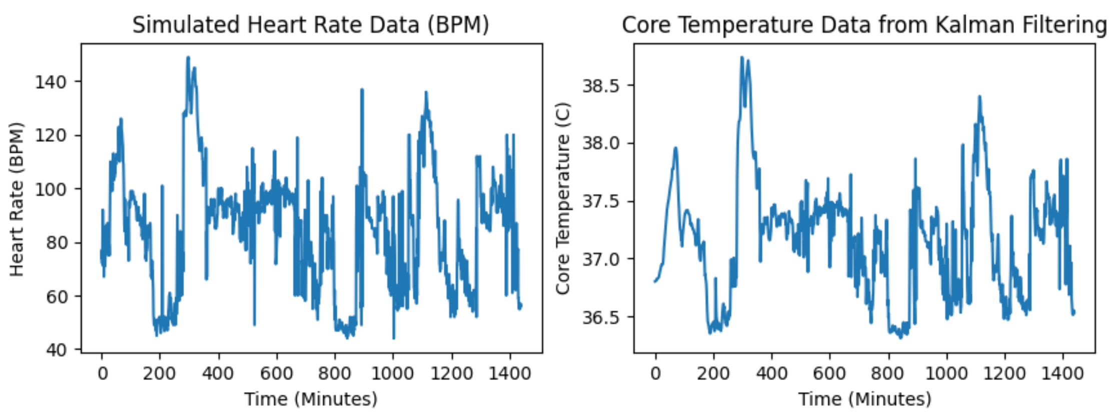

Figure 4: *Graphs generated from proof of concepts taken from two papers.*

	Simulated Heart Rate Data (BPM)	Core Temperature Data from Kalman Filtering
Standard Deviation	21.96673165897368	0.486348738346954
Root Mean Square (RMS)	87.81581461867681	37.163442893767545
Noise Component (STD of Noise)	7.463609123766638	0.12577658585370896
Noise Component (RMS of Noise)	7.463609123766638	0.12577658585370896

Figure 5: *Table that quantifies the noise for each graph.*

Our implementation followed somewhat closely to the model described in Paper 1 (Ezequiel Juarez Garcia et al., 2022). This model allowed us to simulate heart rate data using a Gaussian method and apply a Kalman filter to estimate core body temperature over time. The Kalman filter works by iteratively updating estimates of the system's state (in this case, the CBT) based on noisy measurements (heart rate data in this case) and a prediction model.

The code implementation followed six key steps:

- Initialize core temperature and variance: We initialized the first values of the CBT and variance (v_t) based on the data.
- Estimate core temperature: Using a linear model, we estimated the core body temperature for each time step.
- Estimate variance: We computed the variance for each new estimate, accounting for process noise.
- Compute confidence: The Kalman gain was computed, which helped balance between the prediction from the model and the new measurement from heart rate data.
- Final temperature estimate: The core temperature was updated by combining the Kalman gain with the difference between the predicted and measured values.
- Update variance: The variance was updated based on the Kalman gain and noise in the measurements.

This approach resulted in the generation of the two graphs shown above, where heart rate data was simulated over time and core body temperature was estimated using the Kalman filter. The model successfully reduced noise, as seen in the smoothing of the core temperature data.

After validating the initial model with one-dimensional data (heart rate and temperature). We extended the model to higher dimensions. This involved incorporating additional physiological signals, such as basal body temperature and respiratory rate (BBT and RR), into the filtering process. These signals were modeled with higher-dimensional matrices, which allowed us to account for interactions between different biological clocks in the body.

To manage the phase changes between different rhythms, we introduced rotation matrices into the Kalman filtering algorithm. Rotation matrices are particularly useful when modeling phase changes, such as the shifting of circadian rhythms due to external cues (e.g., light exposure). By incorporating these matrices, we improved the graph's shape from increasing in a y=mx+b pattern to closely resembling a sinusoidal function, allowing for more accurate predictions of core body temperature.

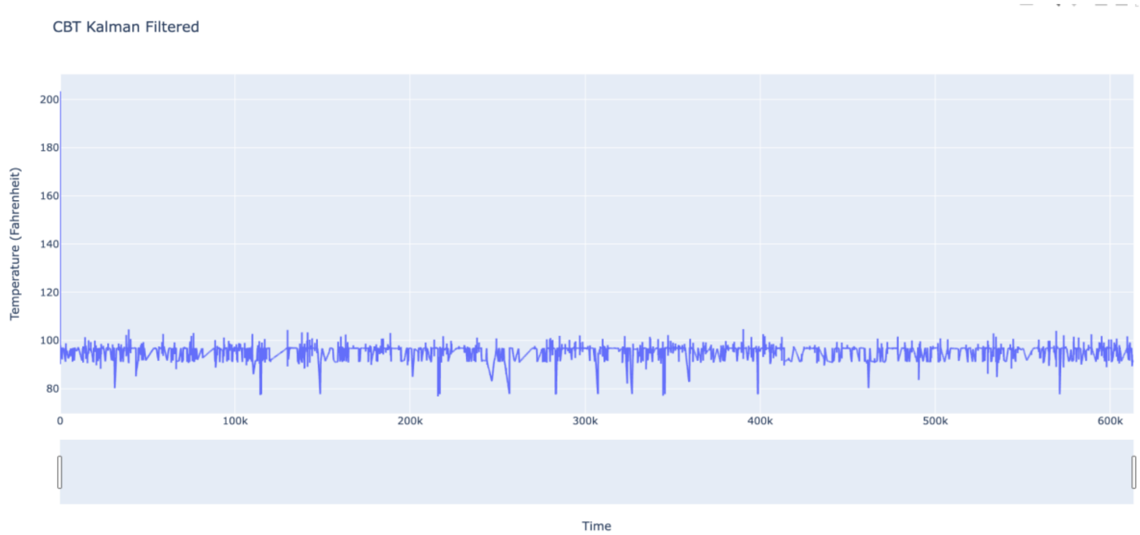

Figure 6: *Initial pattern of the core body temperature Kalman filter*

We decided to tune some specific matrices further to get an accurate pattern to the core body temperature. What we were specifically looking for was that over a 24 hour period, the core body temperature should start off low, then peak at day time, while dropping off at the end of the day. We decided to review literature yet again to identify our gaps in knowledge. To start with, we looked at the P matrix, or the variance matrix. This was a measure of the amount of certainty in the model, and had to be tuned to determine which values are most accurate. Generally, if you are less certain in your model, you should use higher initialization values for this matrix (Welch & Bishop, 2006). As a result, it was initialized to start with the most reasonable values seen in the data for the core body temperature, basal metabolic rate, heart rate, and respiratory rate.

From extensive literature review, it was also decided that the matric Q and R needed to be further tuned as well (process noise covariance and measurement noise covariance matrix respectively). The filterpy library implements a number of Bayesian filters, and we decided to use it. We initialized Q in two different ways to see which one was best suited for us: a version that uses the filterpy library where we took the variance to be 7, and another version that we manually initialized taking the covariances as 0 and the variance (the diagonal elements in the matrix) to be the variances from the data). After testing both, we deduced that the one that used the filterpy library was the closest to taking us to the pattern we wanted to see.

The R matrix in the Kalman filter represents the measurement noise covariance, capturing the error or uncertainty in the measurements. R is represented as:

$$[\sigma^2 \quad \square_{\square\square} \quad \square_{\square\square}]$$
$$[\sigma_{\square\square} \quad \square^2 \quad \square_{\square\square}]$$
$$[\sigma_{\square\square} \quad \square_{\square\square} \quad \square^2]$$

[illegible]

For this project, the R matrix accounts for uncertainties in data collected from the Apple watch, such as basal rate, heart rate, and respiratory rate measurements. Due to the proprietary nature of Apple watch sensors and algorithms, the precise uncertainty for the sensors are unavailable, which required us to take a different approach. The cal_R method was used to estimate R by computing the covariance matrix of the measurement (after they were processed and turned into arrays). R was initialized as:

$$[\sigma^2_{\square\square} \quad \square_{\square\square,\square\square} \quad \square_{\square\square,\square\square}]$$
$$[\sigma_{\square\square,\square\square} \quad \square^2_{\square\square} \quad \square_{\square\square,\square\square}]$$
$$[\sigma_{\square\square,\square\square} \quad \square_{\square\square,\square\square} \quad \square^2_{\square\square}]$$

[illegible]

This approach leverages data variability to approximate measurement uncertainty indirectly, using the inherent spread and relationships within the data. WHile this provided us with a baseline to get R initialized, it could be improved further by directly measuring the uncertainty of the Apple watch through empirical testing.

A matrix of a Jacobian nature was used to model the state transition matrix F. An example of the initial matrix for a three state model is as follows:

$$\begin{bmatrix} \frac{\square\square 1}{\square\square 1} & \frac{\square\square 1}{\square\square 2} & \frac{\square\square 1}{\square\square 3} \end{bmatrix}$$
$$\begin{bmatrix} \frac{\square\square 2}{\square\square 1} & \frac{\square\square 2}{\square\square 2} & \frac{\square\square 2}{\square\square 3} \end{bmatrix}$$
$$\begin{bmatrix} \frac{\square\square 3}{\square\square 1} & \frac{\square\square 3}{\square\square 2} & \frac{\square\square 3}{\square\square 3} \end{bmatrix}$$

This matrix collects partial derivatives of a series of multivariate functions that were derived from fitting the processed sensor data to a sinusoidal function. The first row and column reflect the relationship between the hidden variable (namely core body temperature cycle, sleep cycle, or hunger cycle) and the sensor data acquired from the apple watch. Except for the first row and column cell, which was set at 1, these portions of the matrix were all initialized to zero. For the rest of the rows and columns, the process was more involved due to the presence of ample sample data. The initial values on the diagonals were set to 1, reflecting the direct relationship of each variable to itself. The initial values in the upper and lower quadrants were acquired through first calculating the gradient of each sensor array with respect to time. After this, the mean of the gradient of each variable in a specific cell was computed with respect to the corresponding variable in the column for that row. The constants derived from partial derivation for the entire matrix were then paired with sines or cosines with an omega value of $\frac{\pi}{6}$ that was found to be most optimal for filter tuning because it yielded the most reasonable values when running the Kalman algorithm. Over time, the matrix was adjusted, excluding the constants derived from the partial derivatives, as the filter was run in conjunction with other matrices associated with the Kalman filter process to achieve optimal results.

2.4b Implementation of Kalman Filter for Hunger Levels

In the second model, we are implementing a Kalman filter to process data that is related to energy expenditure to predict our subject's hunger levels throughout the day. For measurement data, we used physical effort data (kcal/hr/kg) and basal energy burned (cal). We hypothesized these measurements had a direct linear relationship to hunger level. With hunger level being an abstract concept in circadian rhythms, we decided to validate our results against the times at which the subject had a meal, assuming peak hunger levels occur at times our subject typically eats meals throughout the day. We observed where our predicted hunger levels reached a local maximum, and if they corresponded with meal times we assumed them to be more accurate or less accurate depending on different models.

For the most part, the procedure we followed to ensemble the subject's physical effort data and the basal energy burned data resembles the procedure to implement the Kalman filter for core body temperature. We again used the model described in paper 1 (Ezequiel Juarez Garcia et al., 2022), ensembling the above two sets of data. The Kalman filter ensemble worked by iteratively updating estimates based on previous system states, and combining them with current measurements—the Kalman gain. The system weights the current measurement with the estimate based on the Kalman gain. Thus, at each step the Kalman filter outputs an estimate of the subject's hunger level.

After extensive literature review, we observed certain numerical relations between each of the input data sets. While we had some information on these relations based on literature, we had to use multiple iterations to find a set of relations that resulted in an output that matched our subject's self-reported hunger and meal times. These relations were codified in the H matrix: each cell in the matrix represents the proportional relationship between the inputs (the previous physical effort measurement, the basal energy burned measurement) and the outputs (the current physical effort measurement, the current basal energy burned, and the output hunger estimate). Ultimately, this matrix controls the relationship between the inputs and the outputs such that the subject's estimated hunger level reaches a maximum when the subject has meals, and then decreases shortly afterwards.

2.4c Adherence to Initial Plan

Our initial goal was to have three estimated cycles from our subject's data (core body temperature, sleep/wake cycles, and hunger levels) that would then be ensembled to form the predicted activity levels of the suprachiasmatic nucleus (SCN). But we soon realized that passing the sleep data, specifically his sleep/wake times, and the type of sleep he had throughout the day would be difficult to manage. Our initial pass of the Kalman filtered sleep/wake cycles made us realize we could simply use the sleep data as a way to validate our predicted SCN activity level graph.

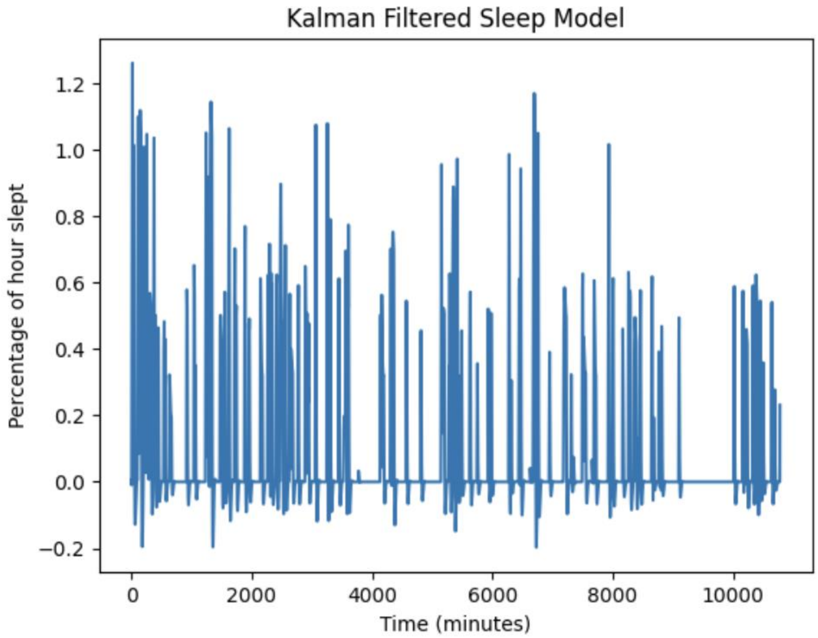

Figure 7: *Initial Kalman filtering of the sleep/wake times data*

3 Results and Discussion

The results of the individual biological clocks for one day using Kalman filtering are as follows, for core body temperature and hunger levels, respectively:

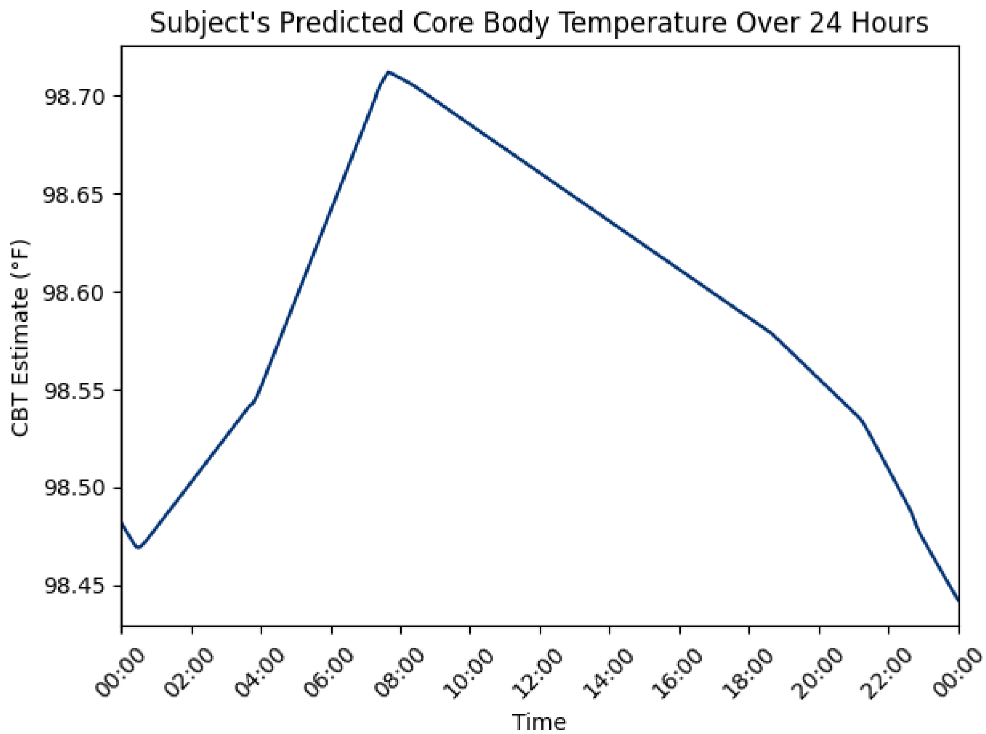

Figure 8: *Predicted Core Body temperature over 24 hours.*

Using the process developed in section 2.4a, the following core body temperature plot was generated through the fusion of Apple Watch sensor measurements of basal metabolic rate, heart rate, and respiratory rate with a hidden variable representing body temperature over time. Results were compared to literature, such as a study by Rossi et al., in order to validate their reasonability and accuracy (Rossi et al., 2001). The subject's predicted core body temperature follows an expected pattern of increasing during the day, reaching a peak of 98.7, and dropping off as the day goes on. The values fluctuate around a mean value of 98.6 degrees Fahrenheit.

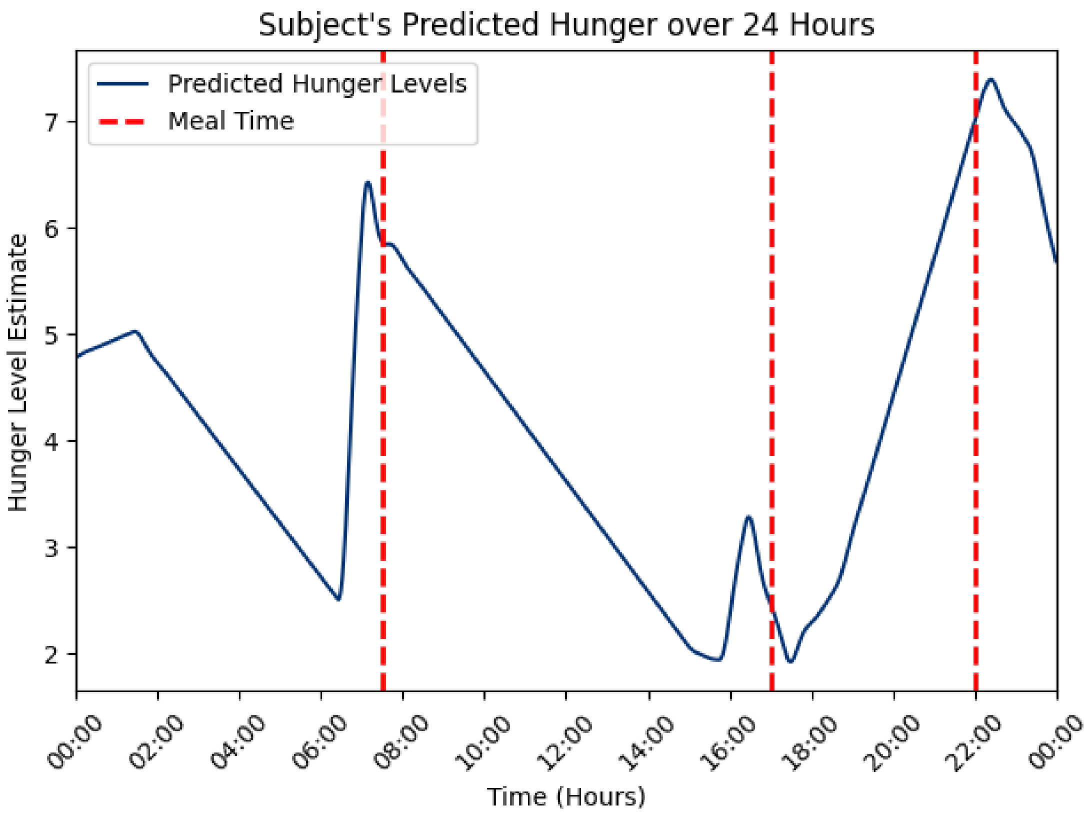

Figure 9: *Predicted Hunger over 24 hours*

Using the process developed in section 2.4a, the following hunger level plot was generated through the fusion of Apple Watch sensor measurements with a hidden variable representing hunger levels for a 24-hour period. The hidden variable was estimated using the sensor data to capture fluctuations in hunger levels. This was then validated against the subject's self-report of hunger times during the specific day studied and delineated in the graph. (Beaulieu & Blundell, 2021).

The y-axis values are arbitrary and represent a composite scale derived from the y-axes of the sensor data used in the analysis. This scale approximately ranges from 2 to 7, where 2 indicates a complete lack of hunger and 7 signifies high hunger levels, as defined by the subject's self-reported experiences. Although the scale does not correspond to a standard measurement, it serves as a normalized representation of the combined sensor outputs. By integrating these values with the hidden variable, the graph illustrates fluctuations in hunger levels over time. This approach enhances sensitivity to sensor-detected variations while reducing noise in the sinusoidal curves. As a result, hunger levels and their underlying patterns can be meaningfully interpreted within the constraints of the available data.

The data from these two plots was ensembled, filtered, and superimposed over sleep data to get the following proof-of-concept approximation of SCN activity:

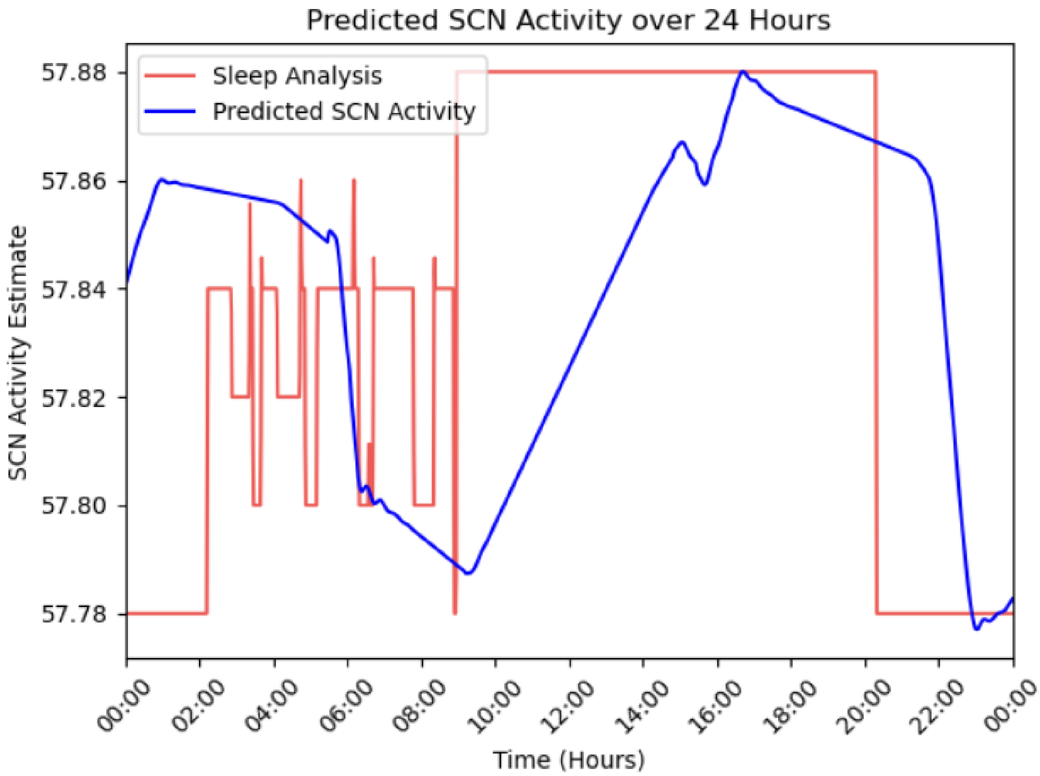

Figure 10: *Predicted SCN activity over 24 hours*

4 Conclusion and Future Plans

Future plans for the project focus on refining various components of the Kalman filtering model and addressing key challenges to improve its accuracy and generalizability. Key areas of enhancement include further tuning the system's matrices, such as refining the measurement uncertainty matrix (R) to better account for Apple Watch errors, and testing the process noise covariance matrix (Q) for optimal values. Special attention will be given to optimizing the HHH and FFF matrices to better represent the cyclical patterns inherent in circadian rhythms. A major focus will also be on implementing a proper validation system to quantify the model's accuracy, potentially through residual analysis, which could help in refining the matrices. To enhance the model's adaptability across different subjects, the extended Kalman filtering framework will be further tuned to ensure its robustness and generalizability and prevent overfitting for one specific person or set of data. The ultimate objective of this project is to create a versatile model capable of integrating various types of biological data—such as the menstrual cycle, androgen cycle, or cellular cycle—into a cohesive ensemble. Achieving this will require standardizing the lower-order Kalman filters and clearly defining the types of data collected to improve consistency and reliability. Addressing overfitting is another critical goal, as the current model has been developed using data from a single test subject. To mitigate this, the project will expand its scope by incorporating data from a more diverse range of subjects and biological variables. This will help ensure that the final model is not only accurate but also broadly applicable to different contexts and populations.

Bibliography

Asgari-Targhi, A., & Klerman, E. B. (2019). Mathematical modeling of circadian rhythms. *WIREs Systems Biology and Medicine*, *11*(2), e1439. https://doi.org/10.1002/wsbm.1439

Beaulieu, K., & Blundell, J. (2021). The Psychobiology of Hunger – A Scientific Perspective. *Topoi*, *40*, 1–10. https://doi.org/10.1007/s11245-020-09724-z

Bieda, R., Grygiel, R., & Galuszka, A. (2015). Naive Kalman filtering for estimation of spatial object orientation. *2015 20th International Conference on Methods and Models in Automation and Robotics (MMAR)*, 955–960. https://doi.org/10.1109/MMAR.2015.7284007

Juarez Garcia, E., Ferguson, D. P., & Napoli, N. J. (2021). Estimating Core Body Temperature Under Extreme Environments Using Kalman Filtering. In *AIAA SCITECH 2022 Forum*. American Institute of Aeronautics and Astronautics. https://doi.org/10.2514/6.2022-1271

Garcia, E. J., Stephens, C., & Napoli, N. J. (n.d.). Detecting High-Risk Anomalies in Aircraft Dynamics Through Entropic Analysis of Time Series Data. In *AIAA AVIATION 2022 Forum*. American Institute of Aeronautics and Astronautics. https://doi.org/10.2514/6.2022-3257

Rossi, S., Zanier, E. R., Mauri, I., Columbo, A., & Stocchetti, N. (2001). Brain temperature, body core temperature, and intracranial pressure in acute cerebral damage. *Journal of Neurology, Neurosurgery & Psychiatry*, *71*(4), 448–454. https://doi.org/10.1136/jnnp.71.4.448

Welch, G., & Bishop, G. (2006). *An Introduction to the Kalman Filter*.